Lasers in Manufacturing Conference 2019

Alternative solutions to crack issues considering laser metal deposition in hybrid-additive manufacturing of press tools

Stefan Belitz[a*], Tobias Todzy[a], Christoph Kaminsky[a], Henning Zeidler[b]

[a]*Daimler AG, Mercedes-Benz Werk Sindelfingen, D-71059 Sindelfingen, Germany*
[b]*Institute for Machine Elements, Design and Manufacturing, TU Bergakademie Freiberg, D-09599 Freiberg, Germany*

Abstract

For geometry changes and to repair functional press tool areas, new material is added using a laser metal deposition (LMD) process. During the cooling of the build-up layers, residual stresses occur which can lead to cracks in the bonding zone. Within the scope of this work, alternative solutions to these crack issues besides a variation of process parameters are sought to reliably increase the permissible application height for the LMD process in accordance with the factory standard. Based on process parameters from previous work and production, the influence of a buffer layer, an increased laser spot diameter and hammer peening on crack formation are investigated. Using LMD, test specimens are additively manufactured on a substrate of spheroidal graphite cast iron and examined with regard to their geometric and metallographic quality. A validation is accomplished on the basis of retries and a significant increase of the application height without crack formation is demonstrated.

Keywords: Laser Metal Deposition; additive manufacturing; crack formation; press tools; cast iron

1. Introduction

Driven by customer wishes, the number of offered models in the automotive industry is constantly increasing (Günthner 2007). Against the background of ever-stricter cost targets, new press tools have to be developed and produced. During the sheet metal forming process, large forces are transferred to the pressing tools. As a result, material is progressively removed by wear mechanisms such as adhesion, abrasion and surface shattering (Czichos and Habig 2015). Since a new production of the deformed tools is costly and

* Corresponding author. Tel.: +49-176-30990516; fax: +49-7031-9082754.
E-mail address: stefan.belitz@daimler.com.

time-consuming, a local repair is performed. The laser metal deposition (LMD) process offers an alternative to manual deposition welding for the application of new material to defective areas.

LMD is an additive manufacturing process using a laser beam as heat source for melting a mostly metallic powder material onto a substrate for layer-wise deposition. This process has established itself for repairs and shape changes on materials that are difficult to weld, since the heat input and thus the microstructure of the applied volume can be controlled based on the process parameters. (Poprawe 2005)

The body of a modern car consists mainly of steel sheets of medium to high strength. Spheroidal graphite cast iron is a common tool material for these types of steel in the press tool industry. Cast iron is an iron-carbon alloy widely used in the production of various technical components with complex shapes. This is due to its good castability, machinability, damping properties and low cost (Bargel and Schulze 2012). In spheroidal graphite cast iron, the carbon is precipitated in a spherical form. Due to the low internal notch effect of the graphite spheres, spheroidal graphite cast iron exhibits greater strength and ductility than other cast iron materials. Due to these good mechanical properties, the material is used in many areas of the press tool industry.

Large application heights are required for geometry changes and for the repair of functional press tool areas. During the cooling of the deposited material, stresses occur which can lead to cracks in the bonding zone. In addition to stress-induced cracks, pores can form in the build-up layers. Figure 1 shows typical defect types of the LMD process on spheroidal graphite cast iron. In addition to stress-induced cracks in the edge area of deposited material (a), chipped layers (b) and pores (c) can form in the bonding and build-up

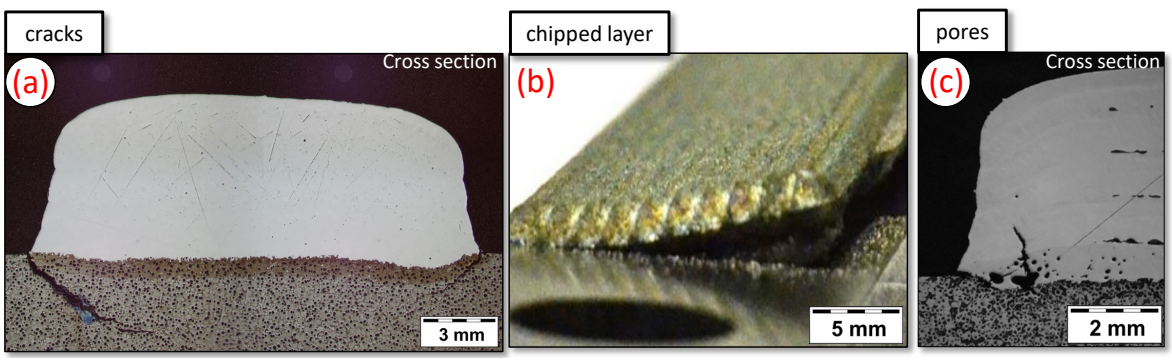

Fig. 1. (a) Stress-induced cracks; (b) chipped layer; (c) pores in build-up layers

zones.

A sizeable amount of literature exists as for the difficulties of LMD on cast iron. Ocelík et al. analyzed the process conditions and layer properties of a LMD-generated cobalt alloy on grey cast iron substrates using a 2 kW Nd:YAG laser and showed that cracking occurs as a result of stresses in the substrate at higher application heights (Ocelík et al. 2007). The crack propagation was observed starting from the outer layer boundary to the inner layer. Xu et al. demonstrate based on two models for the alternating stress of the graphite phases in grey cast iron that the top of precipitated graphite is critical for the formation of microcracks due to tensile stresses (Xu et al. 2014). Lestan et al. investigate the influence of three different powder materials on the microstructure and crack formation in the deposited volume generated by LMD (Lestan et al. 2013). A large number of cracks are detected starting from the bonding zone passing through the martensite zone. The formation of martensite in the heat-affected zone is based on carbon diffusion and high cooling rates. Research shows that graphite precipitates, in which microcracks are usually formed, are dissolved during preheating of the substrate. This reduces the number of microcracks in the bonding zone (Lin et al. 2014). In addition, thermal stresses in the LMD process are reduced. Crack-free coatings are

produced with a substrate that is preheated to a temperature of 600 °C (Jendrzejewski et al. 2006). However, high temperature preheating has disadvantages such as high energy consumption, low productivity and difficult working conditions. Bennett et al. showed that laser deposited repairs of cast iron components can be performed without cracks utilizing the current capabilities of a LMD machine to implement spiral preheating and reheating passes before and after the deposition to control the heating and cooling rate (Bennett et al. 2018).

In this work, a targeted preheating of the substrate is to be achieved by an increased laser spot diameter. Furthermore, the influence on crack formation of methods known from manual build-up welding, is investigated. The cracking resulting from residual tensile stresses can be reduced or avoided by introducing mechanically generated residual compressive stresses in marginal areas close to the surface (Fahrenwaldt et al. 2014). This enables greater shrinkage stresses to be generated before cracking occurs. Within the scope of this work, the application of residual compressive stresses by hammer peening is analyzed. Inhibiting the diffusion of carbon elements into the deposited layer is another effective way to prevent the formation of cracks in the bonding zone (Li et al. 2019). To compensate the residual welding stresses that occur, the buffer layer must be tough and enable plastic behavior. In addition, the carbon diffusion and consequently the hardening of the deposited material is inhibited by nickel. In this paper, a buffer layer is generated to compensate for residual welding stresses and to prevent carbon diffusion. The aim of this work is to reliably increase the by factory standard permissible total layer height for the LMD process to ≥ 5 mm. The deposited layers should be free from cracks and pores in the bonding and build-up zone.

2. Experimental procedure

2.1. Materials

Spheroidal graphite cast iron EN-GJS-HB265 with a hardness range of 220–270 HB 30 and an average tensile strength of about 675 MPa was used as the substrate material in this research. In principle, a powder material of the same type as the base material is used for LMD (Fahrenwaldt et al. 2014). In order to minimize process-related welding residual stresses, attention is paid to a low coefficient of thermal expansion and a high deformation capability when selecting the powder materials. Due to high mechanical quality values and good welding properties, iron-nickel powder materials are recommended for LMD on spheroidal graphite cast iron (Schulze 2010) and therefore are investigated in this work. The metal powders used in the experiment were 3.33 LOWC, Powderfort P and Ferro 702 with size distribution of 45–150 µm, 45–125 µm and 50–150 µm respectively. The chemical compositions of the deposited material and substrate are listed in Table 1.

Table 1. Composition of substrate and powders used for laser metal deposition work

	C	Si	Cr	Mn	Fe	Ni	Mo	Co	Ti	P	S	Cu
3.33 LOWC	0,2	1,2	28	1	Bal.	16	4,5					
SW Powderfort P	0,02				Bal.	18	5	10	1,0			
Plasweld Ferro 702	0,03				Bal.	18	4,8	9,5	1,0			
EN-GJS-HB265 cast iron	3,6	2,05		0,55	Bal.	0,8	0,5			0,04	0,01	1,0

2.2. Methods

The majority of LMD experiments were performed on a multifunctional laser beam hardening and cladding system (HARD+CLAD, produced by ERLASER®). A continuous wave diode laser (LDF400-4000, produced by Laserline GmbH) with a wavelength of 905-1080 nm and maximum power of 4000 W was used for the research work. The diameter of the focal spot on the substrate was kept at 3.3 mm. The laser head and the 3-jet powder nozzle (3-JET-SO12-S, produced by Fraunhofer ILT) were attached to a 6-axis robot system (KR 480 R3330 MT, produced by KUKA). In this work, argon gas was used to protect the molten pool and for powder delivery. A powder feed unit (PF 4/4, produced by GTV company) provided the powder mass flow. The collimation and focusing focal length used were 105 mm and 350 mm respectively. The deposition was prepared on the flat substrates of spheroidal graphite cast iron with dimensions of 520 mm x 600 mm x 40 mm. Volumes with dimensions of 180 mm x 45 mm 5 mm were deposited using a meandering movement of the laser head and different layer structures.

The experiments regarding the influence of a buffer layer and machine hammer peening were based on the following process parameters used in production: laser power of 1100 W, a scanning speed of 360 mm/min, a hatch distance of 50% of the track width and a powder mass flow of 12 g/min.

In order to investigate the influence of a buffer layer on crack formation, the powder materials SW-Powderfort-P from DEW and UTP PlasWeld Ferro 702 from voestalpine were used as alternative materials for the first layer. The remaining four layers were built with 3.33 LOWC.

The induction of residual compressive stresses using a pneumatic hammer was regarded as further alternative solution for reducing the tensile stresses caused by LMD. At the beginning, a deposited volume was generated as reference without hammer peening. Either only the first weld layer or each of the five layers were hammer peened. The LMD process had to be interrupted for hammer peening so that the laser cell could be entered without any safety risks.

Since it is not possible to modify the laser system used for production at Daimler AG, the tests to increase the laser spot diameter were performed in an external application laboratory. Two laser beam sources (LDF 6000-40 and LDF 12000-100, produced by Laserline GmbH) were selected for the experiments. A 3-axis CNC system from Siemens was used for positioning the laser head and implementing the programmed scanning speed v_V. The required powder mass flow $\dot{m}_P$ was provided by the powder feed unit (PF 2/2, produced by GTV company) and transferred to the three-jet powder nozzle (3-JET-SO16-S, produced by Fraunhofer ILT) with a working distance of 16 mm. To increase the laser spot diameter d_S to up to 5.6 mm, the laser process parameters were adjusted accordingly: laser power P_L = 1400 - 2800 W, scanning speed v_V = 720 - 1080 mm/min, powder mass flow $\dot{m}_P$ = 14 - 29 g/min.

2.3. Characterization

After the experiments, the specimens were sectioned using a water jet cutting machine, and then ground, polished and etched with 3 % Nital solution. The microstructure analysis was performed on longitudinal sections and cross sections of the specimens. Characterization of geometric quantities, heat-affected zone and possible defects was observed and analyzed using an optical microscope (OM).

For crack measurement, several support points were placed along a polygon line between the start and end points of a crack. For each deposited specimen, the crack length was measured in two longitudinal and two cross sections. The largest value of the measured crack length was then plotted in diagrams. The porosity was determined graphically using the Stream Enterprise software from Olympus Soft Imaging Solution GmbH.

For the measurement of the powder particle density a sample of the material was taken, embedded,

manually ground and polished. For the analysis, images were generated using an OM and a scanning electron microscope (SEM). The evaluation of the powder particle density was preformed using the OLYMPUS StreamMotion software.

3. Results and discussion

3.1. Hammer peening

In order to investigate the influence of hammer peening on crack formation, all five layers or only the first layer were hammer peened using a pneumatic hammer. To enable a comparison with the current situation, the parameter sets used in production were investigated. Therefore, standard, pyramidal and enlarged first layer structures were analyzed. Figure 2 shows the dependence of the total layer height and crack length in longitudinal and cross sections on different hammer peening methods.

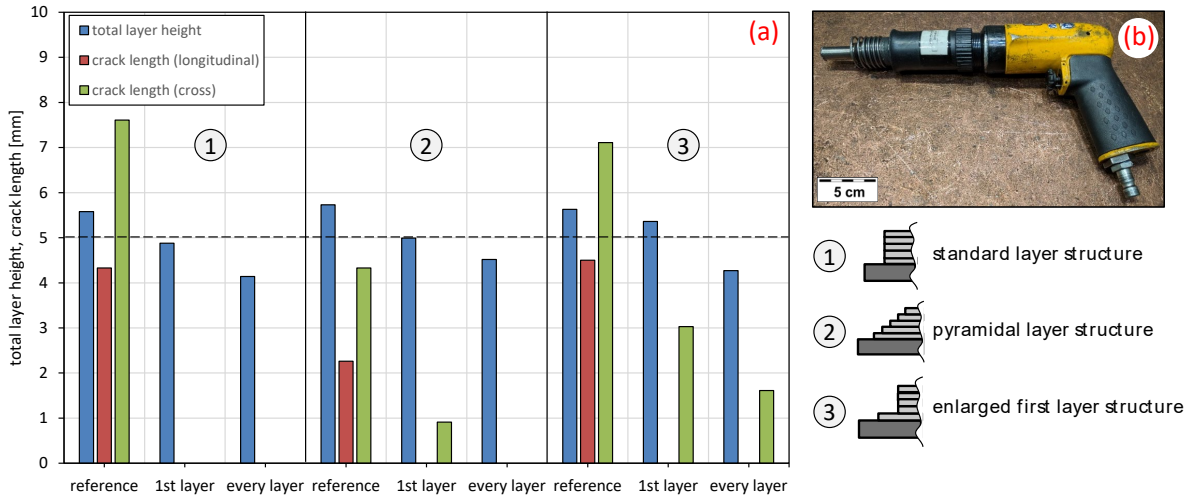

Fig. 2. (a) Dependence of total layer height and crack length on different machine hammer peening variants; (b) pneumatic hammer

With each parameter set, a reference volume was generated at the beginning without hammer peening. As expected, the target total layer height of ≥ 5 mm (shown as dotted line) was reached with each layer structure. In addition, cracks in the longitudinal and cross sections were measured for each reference volume. All cracks measured in the cross section are larger than the cracks of the longitudinal section. When considering the deposited volumes produced with standard layer structure, no cracks are visible in the longitudinal or cross section. The total layer height is reduced from 5.58 mm (reference) to 4.88 mm (1st layer hammer peened) or 4.14 mm (each layer hammer peened) after hammer peening all layers with a pneumatic hammer (see Figure 2, (b)). Using the pyramidal layer structure, a significant influence of hammer peening on crack formation is determined. No crack is observed in longitudinal section after hammer peening the first layer. A crack with a length of 0.91 mm is measured in the cross section. In comparison to the reference volume, this corresponds to a reduction of the cross crack length by 79 %. By using the pyramidal layer structure and hammer peening each layer a crack-free volume was deposited. For deposited volumes with an enlarged first layer, no cracks are measured in the longitudinal section after the first layer or all layers have been hammer peened. The crack length in the cross section is reduced from 7.11 mm (reference) to 3.03 mm (first layer hammer peened) or 1.61 mm (each layer hammer peened).

3.2. Buffer layer

During the deposition of the buffer layer, an unsteady LMD process with large spatter formation is observed. Based on the metallographic analysis of the deposited volumes it is shown that with all examined parameter sets a crack-free volume is generated in longitudinal and cross section. Figure 3 shows the longitudinal sections of two deposited volumes. The buffer layer of the left volume is generated with the powder material PLASweld Ferro 702 from voestalpine. The powder material of the buffer layer shown on the right is SW-Powderfort-P from DEW.

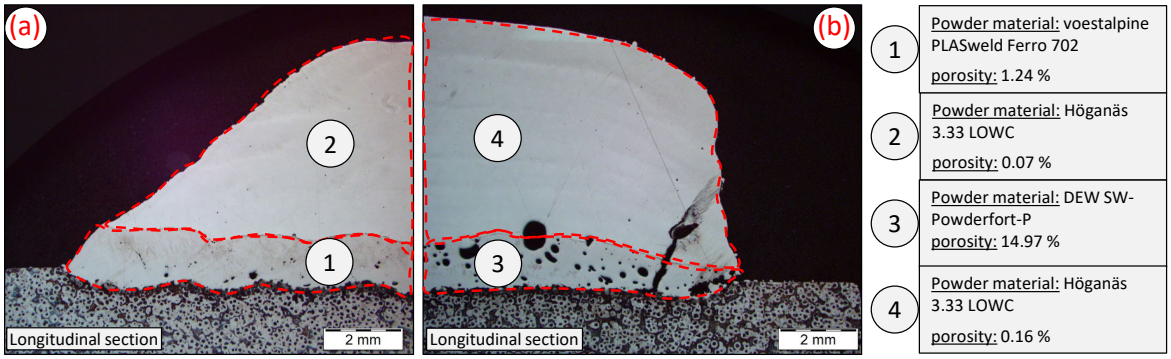

Fig. 4. (a) Longitudinal section of deposited volume with buffer material Ferro 702 (b) longitudinal section of deposited volume with buffer material Powderfort-P

Considering both deposited volumes, a significant difference between the buffer layer and the remaining layers in terms of metallographic quality becomes visible. A parameter variation did not reduce the porosity of the buffer layer. For this reason, it is assumed that the high porosity of the buffer layer was caused by poor quality of the powder materials. Therefore, detailed powder analyses were performed for the powder materials SW-Powderfort-P and PLASweld Ferro 702. Figure 4 shows OM images ((a), (c), (e)) and SEM images ((b), (d), (f)) of the used powders within this work.

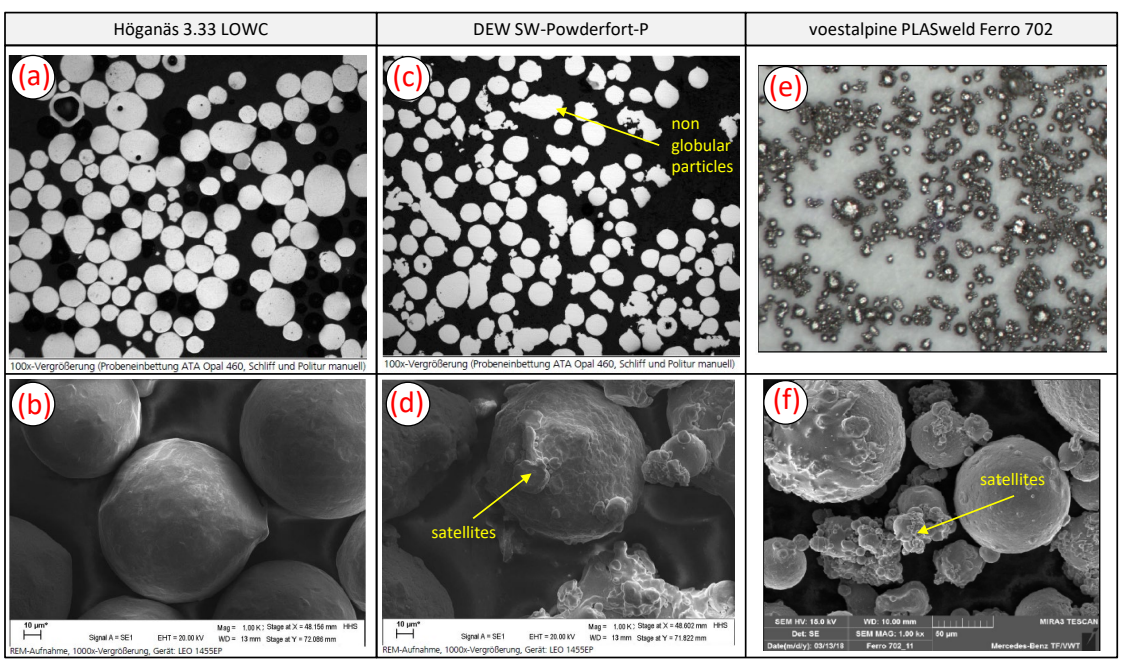

Fig. 3. (a)-(b) Powder cross section and SEM image of 3.33 LOWC; (c)-(d) Powder cross section and SEM image of Powderfort-P; (e)-(f) OM image and SEM image of Ferro 702

The powder cross sections were produced using an OM at a hundredfold magnification. The SEM images show the powder particles at a thousandfold magnification. The powder particles of 3.33 LOWC are globular and without recognizable particle attachments, so-called satellites.

A comparison of the powder cross sections and SEM images of both powders used for the buffer layer, Powderfort-P and Ferro 702, reveals a great similarity. The powder particles are non-globular with recognizable satellites. Inhomogeneous powder particles can lead to problems regarding the powder feed and the LMD process. For this reason, it is assumed that the reason for the high porosity of the buffer layer at different parameter sets is the low quality of both powder materials.

3.3. Increased laser spot diameter

By a variation of the main process parameters laser power P_L, scanning speed v_S and powder mass flow $\dot{m}_P$, the LMD process is adapted to an increased laser spot diameter d_S. Figure 5 shows single weld tracks with increased laser spot diameters of d_S = 3.8 mm (a), d_S = 4.8 mm (b), d_S = 5.0 mm (c) and d_S = 5.6 mm (d) and the main process parameters used.

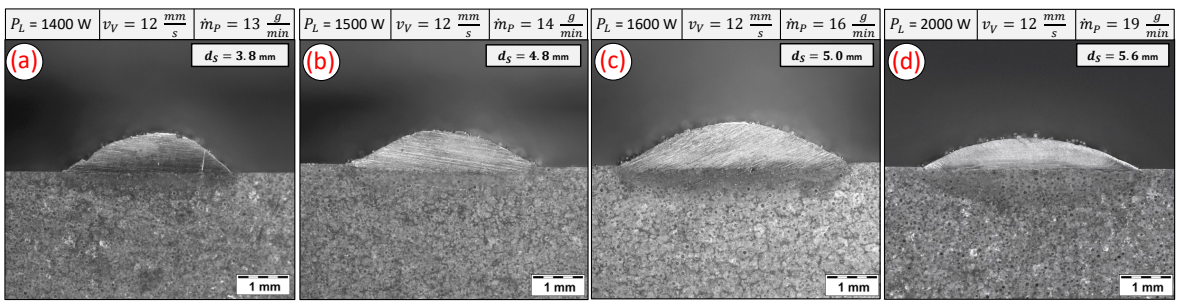

Fig. 5. (a) Single weld track with d_S = 3.8 mm; (b) single weld track with d_S = 4.8 mm; (c) single weld track with d_S = 5.0 mm; (d) single weld track with d_S = 5.6 mm

The single weld tracks shown in Figure 5, (a)-(c), are generated with the laser beam source LDF6000-40. This laser beam source is comparable to the LDF400-4000 laser beam source used at the main plant with regard to the connectable optical fiber and numerical aperture (NA). The LDF12000-100 laser beam source is used to produce the single weld track shown in Figure 5, (d). In order to transfer the results to the available laser system used for production, the laser spot diameter of d_S = 5.6 mm is not considered for further testing. In order to achieve the most extensive preheating of the base material, the laser spot diameter used to generate the individual tracks shown in Figure 5 (c) d_S = 5.0 mm is examined in more detail on the basis of deposited volumes.

To evaluate and check the reproducibility of the test results, the tests are repeated three times and performed with different layer structures used in production. To produce the graphs, the mean value and standard deviation are calculated from the results and plotted in form of an error bar. Figure 6 (a)-(c) shows deposited volumes with three different layer structures in longitudinal or cross section. Figure 6 (d) shows the total layer height for five layers and the crack length in cross and longitudinal section as columns. Below the diagram the investigated layer structures "standard", "pyramidal" and "enlarged first layer" are shown schematically. The dotted line shows the desired total layer height $h_t \geq 5$ mm.

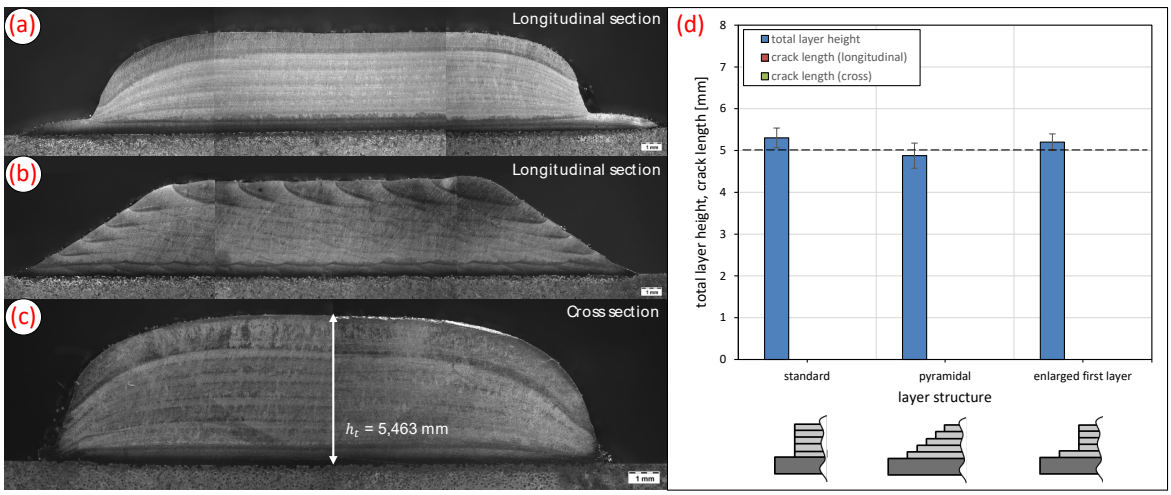

Fig. 6. (a) Deposited volume with enlarged first layer structure; (b) deposited volume with pyramidal layer structure; (c) deposited volume with standard layer structure; (d) total layer height and crack length to validate the results

The target total layer height of $h_t \geq 5$ mm is mostly achieved. With the pyramidal layer structure, the mean value of the total layer height with h_t = 4.88 mm is slightly below the target value. All nine test specimens produced are crack-free in longitudinal and cross section. There are no visible defects in the area of the bonding zone. A stable build-up process is observed in each layer structure and the deposited material is low in porosity.

4. Conclusions and outlook

In this work, alternative solutions to crack issues besides a variation of process parameters considering laser metal deposition were investigated. Test specimens were additively manufactured on a substrate of spheroidal graphite cast iron and examined with regard to their geometric and metallographic quality. The following conclusions can be drawn:

- Deposited volumes hammer peened using a pneumatic hammer are crack-free in longitudinal and cross sections.
- The deposited volumes generated with a buffer layer are crack-free in longitudinal and cross sections. However, a high porosity of the buffer layer is measured as a result of poor powder material quality, regardless of the parameter set selected.
- By increasing the laser spot diameter to 5.0 mm, crack-free deposited volumes are produced. By means of various layer structures and repeat tests it is shown that the total layer height using LMD with a laser spot diameter of 5.0 mm can be reliably increased to ≥ 5 mm.

Within further investigations the alternative solutions should be combined and analyzed with regard to crack formation at total layer heights > 5 mm.

Acknowledgements

The work in this paper was carried out within the scope of the research and development project "ProLMD", which is funded by the German Federal Ministry of Education and Research (BMBF) within the "Additive Manufacturing - Individualized Products, Complex Mass Products, Innovative Materials" (ProMat_3D) Program and implemented by the Project Management Agency Karlsruhe (PTKA). The author is responsible for the content of this publication.

References

Bargel, H.-J.; Schulze, G., 2012. Werkstoffkunde 11. Aufl. Berlin: Springer

Bennett, J.; Dudas, R.; Jian, C.; Ehmann, K.; Hyatt, G., 2016. "Control of heating and cooling for direct laser deposition repair of cast iron components", International Symposium on Flexible Automation. Cleveland, Ohio, U.S.A.

Czichos, H.; Habig, K.-H., 2015. Tribologie-Handbuch. Wiesbaden: Springer

Fahrenwaldt, H. J.; Schuler, V.; Twrdek, J., 2014. Praxiswissen Schweißtechnik 5. Aufl. Wiesbaden: Springer

Günthner, W. A., 2007. Neue Wege in der Automobillogistik. Die Vision der Supra-Adaptivität. Berlin: Springer

Jendrzejewski, R.; Śliwiński, G.; Krawczuk, M.; Ostachowicz, W., 2006: Temperature and stress during laser cladding of double-layer coatings, Surface and Coatings Technology 201 (6), pp. 3328–3334

Lestan, Z.; Milfelner, M.; Balic, J.; Brezocnik, M.; Karabegovic, I., 2013. Laser deposition of Metco 15E, Colmony 88 and VIM CRU 20 powders on cast iron and low carbon steel, International Journal of Advanced Manufacturing Technologies 66 (9-12), pp. 2023–2028

Li, Y.; Dong, S.; Yan, S.; Li, E.; Liu, X.; He, P.; Xu, B., 2019. Deep pit repairing of nodular cast iron by laser cladding NiCu/Fe-36Ni low-expansion composite alloy, Materials Characterization 151, pp. 273–279

Lin, C.-M.; Chandra, A. S.; Morales-Rivas, L.; Huang, S.-Y.; Wu, H.-C.; Wu, Y.-E.; Tsai, H.-L, 2014. Repair welding of ductile cast iron by laser cladding process: microstructure and mechanical properties, International Journal of Cast Metals Research 27 (6), pp. 378–383

Ocelík, V.; de Oliveira, U.; de Boer, M.; de Hosson, J. Th. M., 2007. Thick Co-based coating on cast iron by side laser cladding: Analysis of processing conditions and coating properties, Surface and Coatings Technology 201 (12), pp. 5875–5883

Poprawe, R., 2005. Lasertechnik für die Fertigung. Grundlagen, Perspektiven und Beispiele für den innovativen Ingenieur. Berlin: Springer

Schulze, G., 2010. Die Metallurgie des Schweissens. Eisenwerkstoffe - nichteisenmetallische Werkstoffe 4. Aufl. Heidelberg: Springer

Xu, P. Y.; Liu, Y. C.; Yi, P.; Fan, C. F.; Li, C. K., 2014. Research on variation and stress status of graphite in laser cladding process of grey cast iron, Materials Science and Technology 30 (14), pp. 1728–1734